# A HYBRID SEGMENTATION FRAMEWORK USING LEVEL SET METHOD FOR CONFOCAL MICROSCOPY IMAGES

Quan Xue[1], Severine Degrelle[2], JuhuiWang[1], Isabelle Hue[2] and Michel Guillomot[2]
[1]*INRA, MIA-jouy, Lab. of Applied Mathematics and Informatics, Jouy en Josas F-78350, France*
[2]*INRA, UMR 1198; ENVA; CNRS, FRE 2857, Biologie du Développement et Reproduction, Jouy en Josas F-78350, France*

Keywords: Confocal microscopy, image segmentation, Level-Set, Fast Marching, Geodesic Active Contour.

Abstract: Based on variational and level set approaches, we present a hybrid framework with quality control for confocal microscopy image segmentation. First, nuclei are modelled as blobs with additive noise and a filter derived from the Laplacian of a Gaussian kernel is applied for blob detection. Second, nuclei segmentation is reformulated as a front propagation problem and the energy minimization is obtained near the boundaries of the nuclei with the Fast-Marching algorithm. For each blob, multiple locally optimized points are selected as the initial condition of the front propagation to avoid image under-segmentation. In order to achieve higher accuracy, a graphical interface is provided for users to manually correct the errors. Finally, the estimated nuclei centres are used to mesh the image with a Voronoi network. Each mesh is considered as a Geodesic Active Contour and evolves to fit the boundaries of the nuclei. Additional post-processing tools are provided to eliminate potential residual errors. The method is tested on confocal microscopy images obtained during trophoblast elongation in ruminants. Experimental results show that cell nuclei can be segmented with controlled accuracy and difficulties such as inhomogeneous background or cell coalescence can be overcome.

## 1 INTRODUCTION

Confocal microscopy imaging is one of the most important technologies used to observe the cellular developmental process. Image segmentation is a major step to interpret the obtained images. Correctly explored, it will provide important information about cellular shape and tissue organisation. Appropriate and automatic image segmentation tools are usually necessary to assist the analysis. However, segmenting confocal images is a complex and laborious task. Several factors might raise difficulties: (1) uneven background: Most of the tissues are fluctuating during the image acquisition and background is rarely uniform; (2) local intensity variation inside a nucleus. Due to imperfect staining during the experiment or intrinsic cellular structure, one nucleus may be split into two or more parts; (3) cell coalescence: Cell over-clustering makes it hard to tell the exact nuclei boundaries.

Many segmentation approaches relating to biological images have been proposed in the literature. Research shows that traditional image segmentation methods such as thresholding, region growing and edge-based approaches (Pitas, 2000) can not be successfully applied to microscopy images. Reported successful methods usually focused on a specific type of images without generality (Wu *et al.*, 2005). Watershed segmentation has been popular and considered as one effective method. Thomas (Thomas and Graham, 2007) modified watershed method to give more accuracy for identifying intracellular structures even in the presence of inhomogeneous background. Wahlby (Wahlby *et al.*, 2004) and Long (Long *et al.*, 2007) used both the intensity and geometry information to appropriately detect nuclei. Those methods are robust but the system is complicated and need more time to adjust and analyse the parameters to give the accurate result according to the characteristics of images. All modified watershed algorithms face over-segmentation phenomena and have to provide post processes to adjust the result, especially on cellular microscopy images with high noise and cell coalescence. Based on partial differential equations and variation models, Solorzano (Solorzano *et al.*, 2001), Chang (Chang *et*



Xue Q., Degrelle S., Wang J., Hue I. and Guillomot M. (2008).
A HYBRID SEGMENTATION FRAMEWORK USING LEVEL SET METHOD FOR CONFOCAL MICROSCOPY IMAGES.
In *Proceedings of the First International Conference on Bio-inspired Systems and Signal Processing*, pages 277-282
DOI: 10.5220/0001065602770282

*al.*, 2007) and Dirk (Dirk *et al.*, 2006) provide another direction by using level set segmentation. The solution is derived by minimizing a global energy function. This method benefits from well founded mathematical theories which allow developers to analyze, understand, improve the existing methods and work in a continuous setting in higher dimensional space.

The paper is organized as follows: Section 2 introduces a hybrid structure supporting quality control. Section 3 illustrates segmentation approaches. The system is evaluated in Section 4. Finally, Section 5 draws a conclusion.

## 2 HYBRID FRAMEWORK

Drawing outlines of cells with a mouse, the result can be regarded as absolutely accurate and objective, but it is a hard work and difficult to repeated. Automatic methods are fast and convenient, but some errors occur. Therefore, the solution for image segmentation is a trade-off between precision and speed. When high accuracy is needed, the system needs interactivity with the analyzer or provides an automatic result with limited errors. To deal with a wide variety of biological microscopy images, a hybrid framework with quality control will be preferable.

We constructed such a hybrid framework combining PED-based level set approaches with selectable interaction which supports automatic and semi-automatic segmentation with a robust error-checking stage, as shown in Figure 1. The nuclei are firstly modelled into blobs with some additive noise and Laplacian of Gaussian (LoG) filter is regarded as a blob-detector. Using gradient information, a front propagation fast marching is applied to segment cellular nuclei. The result can be directly outputted after morphology filter or used to enhance the last result. An interactive module is provided to prevent error propagation and Voronoi meshing is created from those appropriate centres. From cellular shape information, geodesic active contour (GAC) is introduced to refine nuclei boundaries. Post processing methods are added as supplementary module to correct for potential errors.

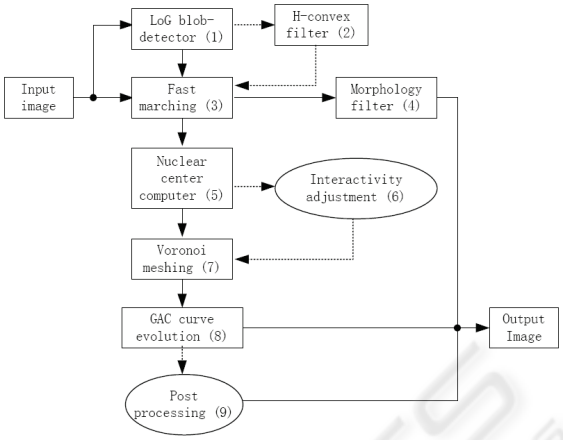


Figure 1: Diagram of hybrid framework.

## 3 METHOD DESCRIPTION

### 3.1 Blob Detection

On confocal images from ruminant trophoblast cells *e.g.* Figure. 2 (A), one sees that most nuclei are nearly round. Laplacian of Gaussian filter has been proved to be an effective blob-detector (Byun *et al.* 2006) since LoG filter is able to detect particular edges by determining the peak point of the ridge. Therefore, we aimed at detecting regions which are brighter than the surrounding to overcome inhomogeneous background.

Although the nuclei of trophoblast cells are not exactly round, our objective is focused on rotation invariance of objects, so that it is fitful to over-fit a circle model into the whole image. From the experimental results, we found that the diameter of LoG filter is proportional to nuclei average diameter and this initial value can be set in advance since the kind of cells are known, e.g. bovine or ovine trophoblast. LoG filter will get a smooth image local maximal values of which nearly correspond to the nuclei centres shown in Figure 2. (B).

After blob-detector, an H-convex filter is added for enhancing the local maximum. H-convex belongs to a kind of morphological method and has the effect of extracting objects that are brighter than background by at least H-intensity units. It is relatively straightforward and does not require homogeneity in the background. The enhanced local maximal result can be gotten in Figure 2. (C).

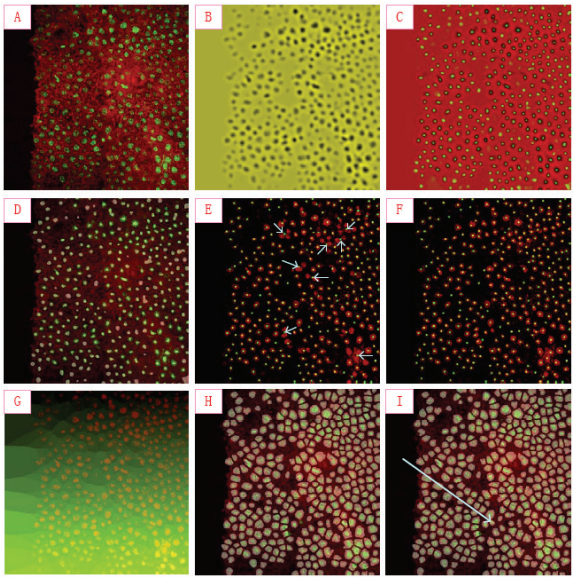


Figure 2: Results in each module.

## 3.2 Fast Marching

Fast marching method (Sethian, 1996) has monotonically advancing front with positive speed to build solutions outward from the boundary condition by choosing the smallest time in its evolution, until it adopts the form of the enclosing nuclei delineated by the staining. The segmentation result from fast marching is gotten in Figure 2 (D).

Our speed function is provided by sigmoid function:

$$S(I') = (Max - Min) \cdot \frac{1}{\left(1 + e^{-\left(\frac{I-\beta}{\alpha}\right)}\right)} + Min \quad (1)$$

where I is intensity of input pixel, $I'$ is the intensity of output pixel, $Min$ and $Max$ are the minimum and maximum values of output image, $\alpha$ defines the width of input intensity range and $\beta$ defines intensity around which the range is centred.

Since some cell nuclei are connected closely, segmentation results depend on initial seed positions, so that multiple seeds will have more chances not to miss objects. However, having seeds distributed inside the nuclei is not helpful for contour expansion. Therefore, instead of randomly selecting multiple points as initial condition, we searched the best seeds for each candidate by finding its local minimum through comparison with neighbours as shown in Figure 3.

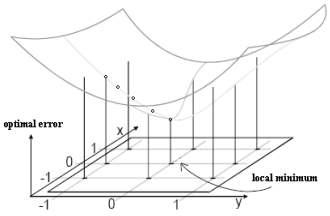


Figure 3: Seeds optimization by local searching.

The selection of optimal seeds gives a better result in detecting nuclei, and that this result is stable shown Table 1. The more seeds can be assigned nearby the edge of nuclei, the more precise the fast marching segmentation can be. Table 1 also shows that the number of initial seeds is important. If too many seeds are put in one image, many single nuclei will be divided into multiple parts due to local intensity variations. Normally the distances we have selected are 16 pixels in row, 16 pixels in column and a searching radius of 3 pixels. For some special trophoblast images we had to adjust these parameters carefully.

Table 1: Comparison between random and optimal seeds.

| radius (pixels) | Number of nuclei | 4×4 | 8×8 | 16×16 | 32×32 | 64×64 |
|---|---|---|---|---|---|---|
| 3 | Optimal | 398 | 360 | 337 | 339 | 310 |
| | Random | 419 | 364 | 332 | 319 | 307 |
| 5 | Optimal | 319 | 312 | 303 | 304 | 302 |
| | Random | 337 | 312 | 299 | 288 | 275 |

## 3.3 Interactivity

The centre of each nucleus can be estimated from the above results. Despite accuracy rate is averagely high, there is still a possibility of a few failures to occur as indicated by white arrows on Figure 2 (E). On our images, the error rate varies from 1% to 10%. If more than one seed is located inside a nucleus, this will cause over-segmentation, conversely when no seed is found within a nucleus, the object is lost. Therefore, the centres of nuclei are very important for the final result. In order to prevent error propagation, human interactivity is necessary to view and adjust results in this stage. Through an interface, the user can make decision based on visual examination of the nuclei, so that an immediate feedback enables the user to produce reliable results e.g. Figure 2 (F).

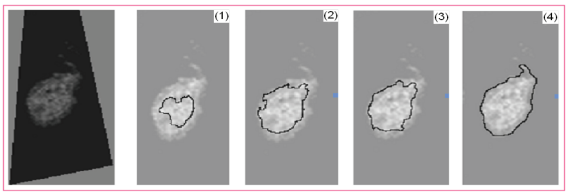


Figure 4: Refinement by GAC in one Voronoi mesh.

### 3.4 Geodesic Active Contour

From nuclei centres, Voronoi mesh is directly produced in Figure 2 (G), which can be regarded as a reference map in refining nuclei by geodesic active contours (Vicent *et al*. 1997). Since Voronoi mesh gives a limited small region to minimize the GAC energy function, it is sure that one nucleus is gotten just in one Voronoi-mesh. The refining result is shown in Figure 2 (H).

GAC consists of double forces which control the last shape and it is important to balance inside and outside forces. When the propagation term is set too high, the contour will go too far inside as illustrated in Figure 4. In our application to ruminant trophoblast cells, all nuclei are nearly rounded so that curvature term is responsible for smoothness.

### 3.5 Post Processing

When confocal images are very blurred or tightly clustered, a few errors cannot be avoided with automatic detection to correct these potential errors by human visual system. We provide a supplementary module. As an example (Figure 2: I), one lost nucleus has been recovered with this module.

## 4 EXPERIMENTS

This section describes how our hybrid framework is used to segment the nuclei on 2D confocal images from ruminant trophoblast. There are more than one thousand of images with varying cellular characteristics and varying background noise in dataset. Selecting different modules, four types of pipeline are designed shown in Table 2.

Table 2: Pipelines with different modules.

| Module | 1 | 2 | 3 | 4 | 5 | 6 | 7 | 8 | 9 |
|---|---|---|---|---|---|---|---|---|---|
| Pipeline A | × | × | × | × | | | | | |
| Pipeline B | × | × | × | | × | | × | × | |
| Pipeline C | × | × | × | | × | × | × | × | |
| Pipeline D | × | × | × | | × | × | × | × | × |

Figure 5 gives four typical images as examples to show the results of our framework. Our approach is compared with the existing methods in ITK and ImageJ which are using fast marching and K-means clustering individually. In row 1, when confocal images have good quality, all methods can be used successfully, with similar errors. However, when nuclei are clustered together (see row 2), our method keeps stable whereas the other methods lose the ability to separate each nucleus in the clusters. For example, ITK can only detect the whole cluster edge and cannot divide it further while ImageJ produces many connected regions. In row 3, when nuclei are organised in a special structure, the exiting methods (ITK and ImageJ) cannot identify the objects whereas the nuclei are correctly detected by our method and the contour is closer to the true shape. When there are many small nuclei and their size changes continuously (row 4), our result is also stable and useful.

Our framework is a scalable system with quality control through the selection of modules and the setting of the initial parameters based on the characteristics of the original image to balance terms in the energy function of level set. Through adjusting the parameters on propagation and smooth term, the nuclear edges can be detected and refined step by step by active contour as in Figure 6, from (a) to (d).

It is often necessary to complete a confocal image automatic segmentation with an acceptable error rate. Successful results can be obtained with our scalable procedure. Since the modules related to the human interaction are selectable, we can use the level set methods directly. Figure 7 gives an example. The first column comes from the fast marching following the blob-detector and we use morphology filter to enhance the result. In the second column, results from GAC without interactivity are provided. Some error is propagated from fast marching module because the gravity centre of the nuclei is wrongly estimated from fast marching segmentation. GAC can skip the false nuclei but will produce good results with coherent nuclei. So, the number of nuclei from GAC decreases for factual objects.

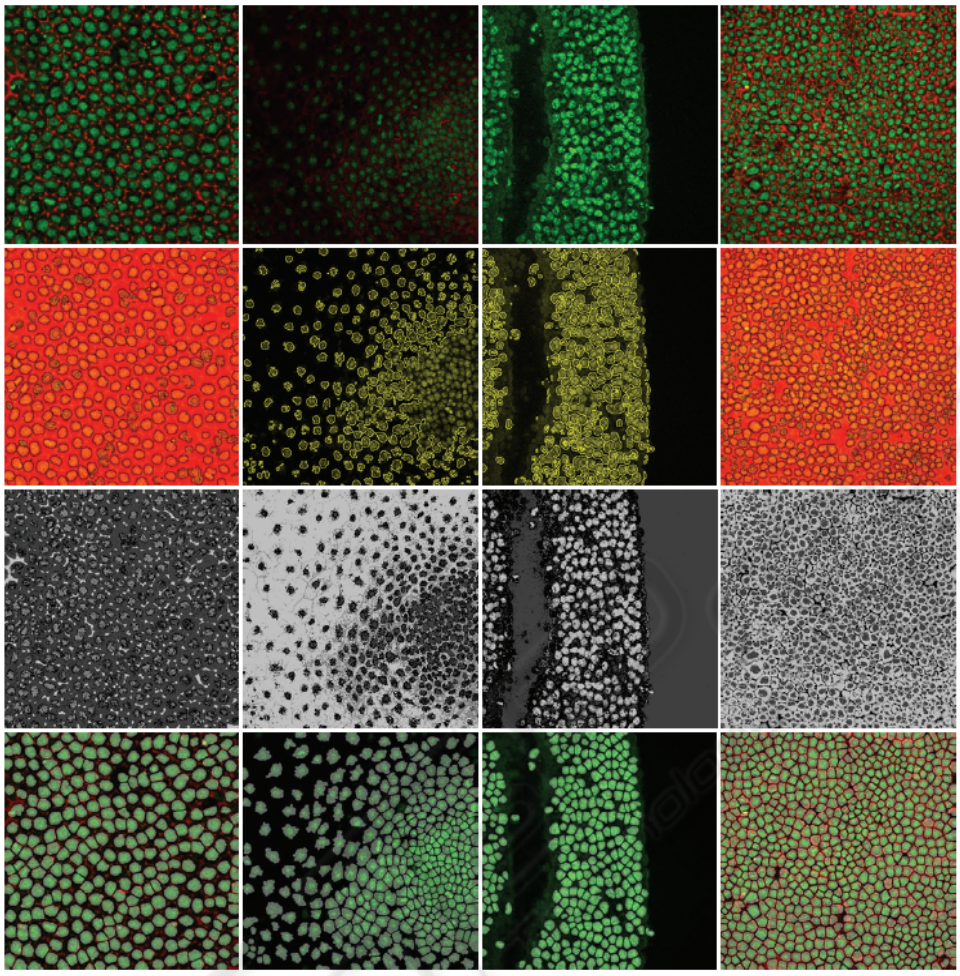

Figure 5: Comparison of proposed algorithm with fast marching in ITK and K-mean clustering in ImageJ (high quality, nuclei coalescence, special structure and low quality from left column to right column). The first row is the original confocal images. The second, the third and the fourth row respectively correspond segmentation results from ITK, ImageJ and proposed algorithm (Pipeline C).

Table 3: Segmentation results expressed as numbers of detected nuclei with each method.

| Image | Actual number | Fast marching in ITK | K-means in ImageJ | FM with blob-detector (Pipeline A) | GAC without interactivity (Pipeline B) | GAC with interactivity (Pipeline C) | With post processing (Pipeline D) |
|---|---|---|---|---|---|---|---|
| (a) | 280 | 253(-27) | 265 (-15) | 298 (+18) | 294 (+14) | 280 (+0) | 280 |
| (b) | 378 | 281(-97) | 347 (-31) | 402 (+24) | 373 (-5) | 374 (-4) | 378 |
| (c) | 294 | 236(-58) | 179 (-115) | 328 (+34) | 318 (+24) | 292 (-2) | 294 |
| (d) | 704 | 544(-160) | 652 (-52) | 737 (+33) | 729 (+25) | 711 (+7) | 704 |
| Number | 1656 | 1314 (-342) | 1443 (-213) | 1765 (+109) | 1714 (+63,-5) | 1657 (+7,-6) | 1656 |
| Error rates | | 20.65% | 12.86% | 6.58% | 4.11% | 0.79% | 0% |

In Table 3, we conclude and compare the error rates from all of the methods discussed above. "+" means over-segmented nuclei and "-" means under-segmented. Their sum is divided by factual total numbers to compute the error rate. Normally we do not use post processing module and the average error ratio is limited into 0.8%. The experimental results show that our hybrid segmentation framework is satisfactorily accurate.

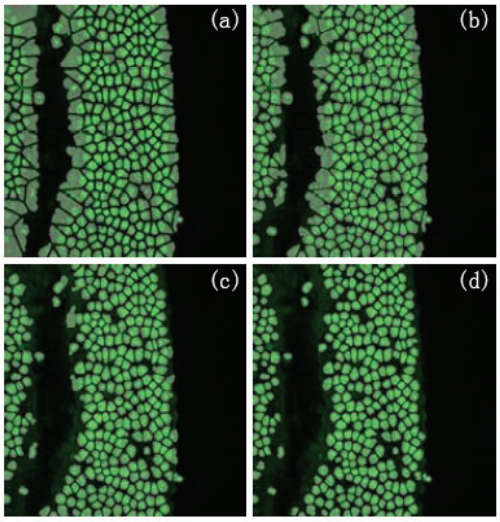


Figure 6: Refining boundary by GAC method with quantity control.

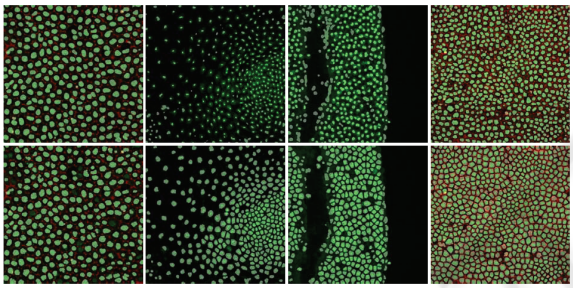

Figure 7: Automatic segmentation results by Pipeline A (first row) and Pipeline B (second row).

## 5 CONCLUSIONS

This paper demonstrates the effectiveness of a hybrid framework for cellular segmentation. It combines the efficiency of the automatic segmentation procedures with the accuracy of the human visual system. Based on confocal images of ruminant trophoblast, our experiments showed that the proposed approach provides reliable results and presents numerous advantages regarding to manual analysis or automatic methods in terms of objectivity and applicability.

## ACKNOWLEDGEMENTS

QX and SD are respectively supported by an INRA and an Ile–de-France post-doctoral fellowship. Scientific financial support comes from an INRA AgroBi grant to JW and IH. We thank A Trubuil P Adenot* and G Lehmann* for helpful discussions (*INRA MIMA2 platform) and INRA experimental farms for embryo production.

## REFERENCES

Byun. J.Y., Verardo. M.R., Sumengen. B., Lewis. G.P., Manjunath. B.S., Fisher. S.K., 2006. Automated tool for the detection of cell nuclei in digital microscopic images: Application to retinal images. *Molecular Vision*, pp.949-960. August 2006.

Chang. H., Park. C., Parvin. B., 2007. Quantitative representation of three-dimensinal cell culture models. In *ISBI'07, IEEE International Symposium on Biomedical Imaging: From Nano to Macro,* pp.536-539. April 12-15, 2007. Washington DC, USA.

Dirk. P., Jens. R, Nick. T., Badrinath. R., 2006. Spatio-Temporal Cell Cycle Phase Analysis Using Level Sets and Fast Marching Methods. In *MIAAB'06, 1st international workshop on Microscopic Image Analysis with Applications in Biology*. On 5th of October 2006. Copenhagen, Denmark, USA.

Long. F.L., Peng. H.C., Myers, E., 2007. Automatic segmentation of nuclei in 3D microscopy images of c.elegans. In *ISBI'07, IEEE International Symposium on Biomedical Imaging: From Nano to Macro*, pp.536-539. April 12-15, 2007. Washington DC, USA.

Pitas. I., 2000. *Digital image processing algorithms and applications.* Wiley-Interscience publication. New York, 1st edition

Sethian, J.A., 1996. *Level set methods and fast marching methods.* CAMBRIDE UNIVERSITY Press.

Solorzano. C.O., Malladi. R., Lelievre.S.A., Lockett. S.J., 2001. Segmentation of nuclei and cells using membrane related protein markers. *Journal of Microscopy*, Vol.201, Pt 3, pp.404-415, March 2001.

Thomas, J.G., Graham, W., 2007. WatershedCounting3D: A new method of segmenting and counting punctuate structures from confocal image data. *Blackwell Synergy - Traffic*, Volume 8 Issue 4 pp. 339-346, April 2007.

Vicent. C., Ron. K, Guillermo. S., 1997. Geodesic Active Contours. *International Journal of Computer Vision*, Vol.22 (1), pp.61-79, 1997.

Wahlby. C., Sintorn. I.M., Erlandsson. F., Borgefors. G., Bengtson. E., 2004. Combining intensity, edge, and shape information for 2D and 3D segmentation of cell nuclei in tissue sections. *Journal of Microscopy,* Vol.215, Pt 1, pp.67-76, July 2004.

Wu. H.S., Xu. R., Harpaz. N., Burstein. D., Gil. J., 2005. Segmentation of intestinal gland images with iterative region growing. *Journal of Microscopy,* Vol.220, Pt 3, pp.190-204, December 2005.